

Microporosity Prediction and Validation for Ni-based Superalloy Castings

This content has been downloaded from IOPscience. Please scroll down to see the full text.

2015 IOP Conf. Ser.: Mater. Sci. Eng. 84 012003

(<http://iopscience.iop.org/1757-899X/84/1/012003>)

View [the table of contents for this issue](#), or go to the [journal homepage](#) for more

Download details:

IP Address: 128.255.19.162

This content was downloaded on 29/06/2015 at 16:06

Please note that [terms and conditions apply](#).

Microporosity Prediction and Validation for Ni-based Superalloy Castings

J Guo¹, C Beckermann², K Carlson², D Hirvo³, K Bell⁴, T Moreland⁴, J Gu⁵,
J Clews⁵, S Scott¹, G Couturier¹ and D Backman⁶

¹ ESI US R&D, Columbia, MD

² Department of Mechanical Engineering, University of Iowa,

³ Alcoa / Howmet, Whitehall, MI,

⁴ PCC Airfoils, Cleveland, OH

⁵ PCC Structurals, Portland, OR

⁶ Backman Materials Consulting, LLC, Saugus, MA

E-mail: jianzhengguo@gmail.com

Abstract. Microporosity in high performance aerospace castings can reduce mechanical properties and consequently degrade both component life and durability. Therefore, casting engineers must be able to both predict and reduce casting microporosity. A dimensionless Niyama model has been developed [1] that predicts local microporosity by accounting for local thermal conditions during casting as well as the properties and solidification characteristics of the cast alloy. Unlike the well-known Niyama criterion, application of the dimensionless Niyama model avoids the need to find a threshold Niyama criterion below which shrinkage porosity forms – a criterion which can be determined only via extensive alloy dependent experimentation. In the present study, the dimensionless Niyama model is integrated with a commercial finite element casting simulation software, which can now more accurately predict the location-specific shrinkage porosity volume fraction during solidification of superalloy castings. These microporosity predictions are validated by comparing modelled results against radiographically and metallographically measured porosity for several Ni-based superalloy equiaxed castings that vary in alloy chemistry with a focus on plates of changing draft angle and thickness. The simulation results agree well with experimental measurements. The simulation results also show that the dimensionless Niyama model can not only identify the location but also the average volume fraction of microporosity distribution in these equiaxed investment cast Ni-based superalloy experiments of relatively simple geometry.

1. Introduction

Porosity formed in castings leads to a decrease in the mechanical properties [2-7]. One of the most effective ways to minimize porosity defects is to design a feeding system using porosity prediction modeling. In such a way, the casting analysis can determine the location and magnitude of porosity such that the feeding system can be redesigned. This process is repeated until porosity is minimized and not likely to appear in the critical areas of the castings.

There are many models which can predict the shrinkage porosity from the pressure drop during inter-dendritic fluid flow and gas evolution [5-12]. As is the case for many casting defects observed in solidification processes, the mushy zone regime is the focus of microporosity formation. The basic mechanism of shrinkage microporosity formation is pressure drop due to shrinkage in the liquid

DISTRIBUTION STATEMENT A: Approved for public release; Distribution is Unlimited. Case Number: 88ABW-2014-5285.



Content from this work may be used under the terms of the [Creative Commons Attribution 3.0 licence](https://creativecommons.org/licenses/by/3.0/). Any further distribution of this work must maintain attribution to the author(s) and the title of the work, journal citation and DOI.

[2][13][5].

The liquid densities of many alloys are lower than that of the solid phase. Hence solidification shrinkage occurs due to the metal contraction during the phase change. The pressure within the liquid decreases because of the contraction and sometimes cannot be compensated by the metallostatic pressure associated with the height of the liquid metal.

Generally speaking, there are two ways to predict the microporosity in castings. One is a parametric method by using a feeding resistance criterion function combined with macroscopic heat flow calculations [7-10]. Parametric models are easy to apply to shaped castings. Another approach is a direct simulation method [5-9][13-15]. The parametric models and/or direct methods usually derive governing equations based on a set of simplifying assumptions and solve the resulting equations numerically. By utilizing the cellular automata technique, some models can not only predict the percentage porosity but also the size, shape and distribution of the pores [10-12].

A simplified porosity model called “POROS=1” was developed by ProCAST[16] to predict piping, macroporosity, and microporosity. This model is excellent in predicting piping and macroporosity but not always effective in predicting microporosity. There are several parametric methods to predict microporosity. Among all parametric methods, the Niyama criterion[17] is the most widely used microporosity evaluation method in metal casting. This criteria proposes that shrinkage porosity will form in regions where Niyama values are below some critical threshold value. This threshold Niyama value normally is an alloy chemistry-dependent unknown determined by experimentation. The volume fraction of porosity cannot be calculated based on Niyama value. Carlson and Beckermann[1] developed a dimensionless form of the well-known Niyama criterion to directly predict the amount of shrinkage porosity with the consideration of both the local thermal conditions as well as the thermal properties and solidification characteristics of the alloy.

In this paper, the dimensionless Niyama model is integrated with the existing POROS=1 model in ProCAST to more accurately predict piping, macroporosity, and microporosity. Such an integrated model is used to predict the location-specific shrinkage porosity volume fraction during solidification of superalloy castings. The predictions are validated by comparing against radiographically and metallographically measured porosity for several Ni-based superalloy equiaxed castings that vary in alloy chemistry with a focus for the current reported effort on plates of changing draft angle and thickness.

2. Model Description

As the integrated model described in this paper is the integration of POROS=1 and dimensionless Niyama, these primary models are briefly reviewed as follows.

2.1. POROS=1 Model

There are three fundamental parameters in the POROS=1 model: *pipefs*, *macrofs*, and *feedlen*. The values of these parameters depend on casting process and alloy. The physical meaning of these parameters are explained in[16]. The first two parameters, *pipefs* and *macrofs* are two critical fractions of solid corresponding to the formation of piping and macroporosity. The third parameter, *feedlen* is a length parameter that determines the feeding ability in the late stages of the solidification process [16]. The detailed description of the model can be found in [16].

2.2. Dimensionless Niyama Model

The dimensionless Niyama is derived based on 1-D directionally solidifying system [1]. Darcy’s law is written for such system as:

$$f_i v_i = -\frac{K}{\mu} \frac{dP}{dx} \quad (1)$$

Where f_l is the volume fraction of liquid phase, v_l is the liquids velocity in the mush, μ is the liquid dynamic viscosity, P is the pressure, x is the spatial coordinate, and K is the mushy zone permeability. The pressure drop can be calculated by:

$$\frac{dP}{dx} = \frac{\mu\beta\dot{T}}{KG} \quad (2)$$

Where $\beta = (\rho_s - \rho_l) / \rho_l$ is the solidification shrinkage, \dot{T} is the cooling rate, and G is the temperature gradient.

Porosity forms when pressure drops below a critical value. With some manipulation, the dimensionless form of Niyama can be written as:

$$Ny^* = C_\lambda \frac{G}{\dot{T}^{5/6}} \sqrt{\frac{\Delta P_{cr}}{\mu\beta\Delta T_f}} = \int_{f_{l,cr}}^1 180 \frac{(1-f_l)^2}{f_l^2} \frac{d\theta}{df_l} df_l \quad (3)$$

Where C_λ is a material constant, ΔT_f is the freezing range, θ is the dimensionless temperature, ΔP_{cr} is the critical pressure drop, and $f_{l,cr}$ is the critical liquid fraction point when porosity forms. The critical liquid fraction can be calculated after Ny^* calculation based on the one-to-one correspondence between the integration of equation (3) and $f_{l,cr}$. Then the porosity will be calculated based on the shrinkage from the critical liquid fraction to complete solidification. Complete details of the Ny^* model can be found in [1].

2.3. Integration of POROS=1 and Dimensionless Niyama Criterion (Ny^*)

POROS=1 provides excellent prediction of piping and macroporosity but has a reduced level of accuracy regarding microporosity. Dimensionless Niyama (Ny^*), on the other hand, exhibits good accuracy in predicting microporosity but not for piping and macroporosity. To fully take advantage of POROS=1 model and dimensionless Niyama, POROS=1 and dimensionless Niyama are now integrated such that POROS=1 is used to predict piping and macroporosity and dimensionless Niyama criterion is used to predict microporosity. The run parameter of *FEEDLEN* in the POROS=1 model is removed. Instead, the microporosity is calculated based on dimensionless Niyama value as described above.

3. Experimental Validation

In order to provide initial validation of the above developed model, several Ni-based superalloy equiaxed castings that have different alloy chemistries (IN718 and Mar-M-247) and tapered plates with different configurations were investment cast. Figure 1 shows the experiment setup. There are 24 test coupons per mold. Each coupon is 8" long and 1.8" wide with various thicknesses (0.060", 0.125", 0.250", and 0.500") and taper angles (0, 5%, 10%, and 15%). For each mold, there are 8 thermocouples, 2 inside the metal and 6 inside the shell. All coupons were X-rayed and the X-Ray images of the castings were digitized and thru thickness porosity levels were determined by detailed image analysis. Some of the test coupons were cut into halves for more detailed metallography and to confirm the X-Ray measured porosity levels.

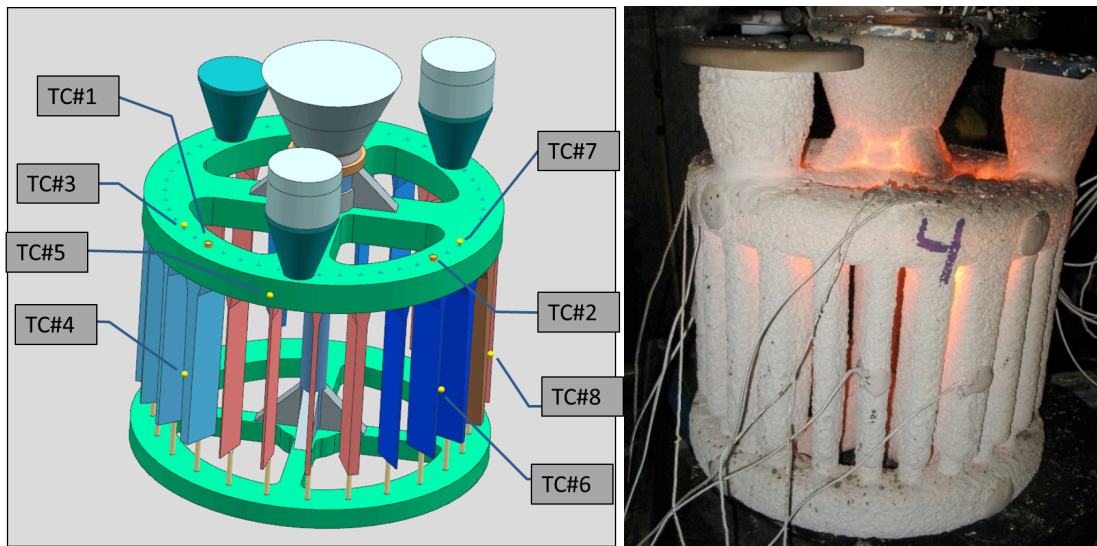


Figure 1. CAD model of the experimental setup (left) and mold with poured liquid metal (right).

Figure 2 summarizes the comparison of predicted and measured microporosity for an IN718 alloy with different wall thickness and plate tapers. In the prediction, $\Delta P_{cr} = 4$ bars. In the figure, the top image of each pair shows the digitized X-Ray measured porosity from the experimental casting. The bottom images show the porosity evaluation from the casting simulation model using the integrated POROS=1 and dimensionless Niyama (Ny^*) model. For a given taper angle, porosity level decreases with increasing thickness. For a given thickness, porosity decreases with increasing taper angle.

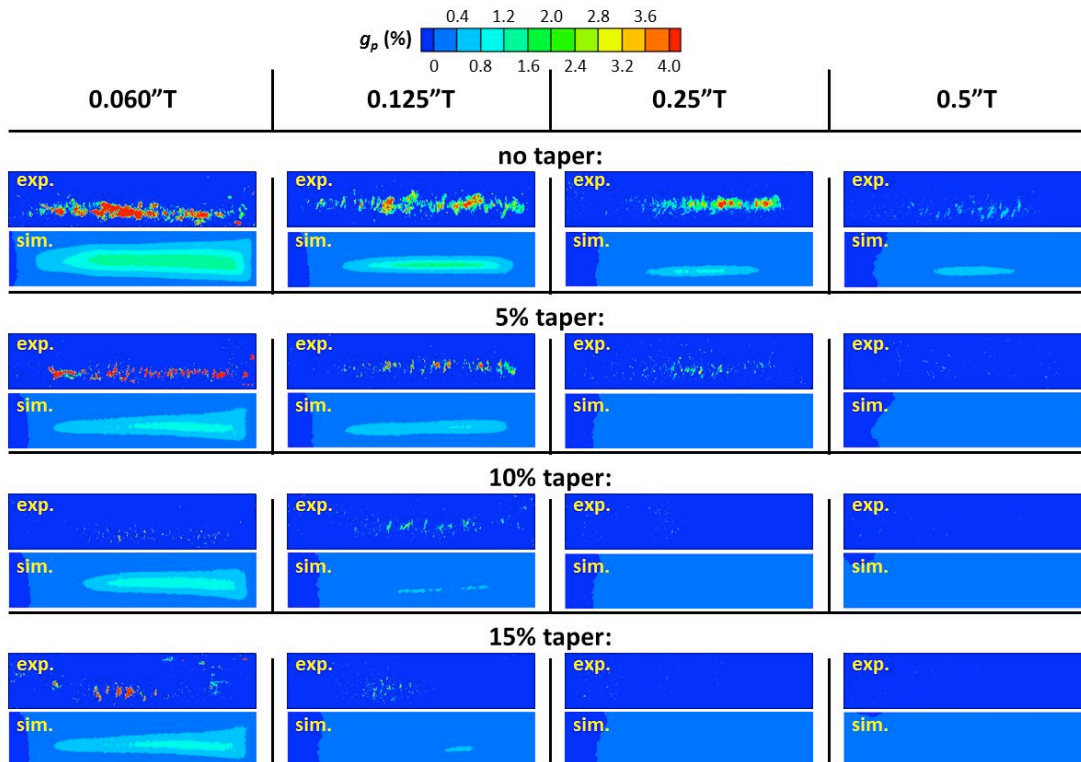


Figure 2. Comparison of prediction and measurement of porosity for different wall thickness and plate taper angles.

There are several adjustable variables in equation 3, such as the critical pressure drop ΔP_{cr} and the critical liquid fraction $f_{l,cr}$. Those variables can be adjusted to better match the experiment measurement. For example the effect of the critical pressure drop on the prediction against the experiment measurement for non-tapered plates can be found in figure 3. Error bars in the figure indicate uncertainty determined from duplicate plates. Compared to the experiment, the model can predict the trend of micro-porosity very well. For the alloy studied here, $\Delta P_{cr}=4$ bars gives the best match.

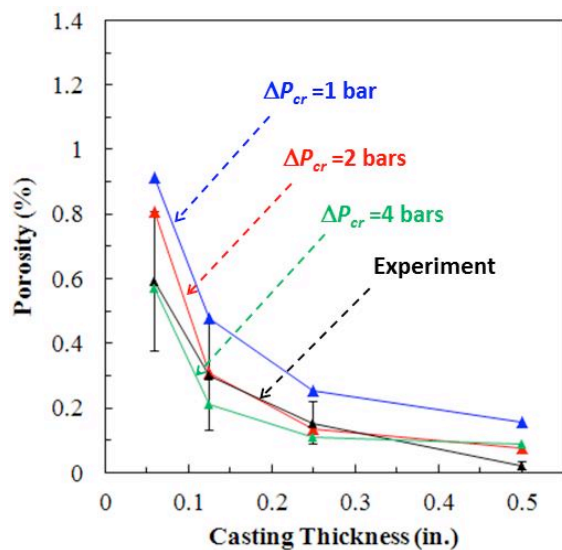


Figure 3. Comparison of porosity between simulation and experiment for non-tapered plates.

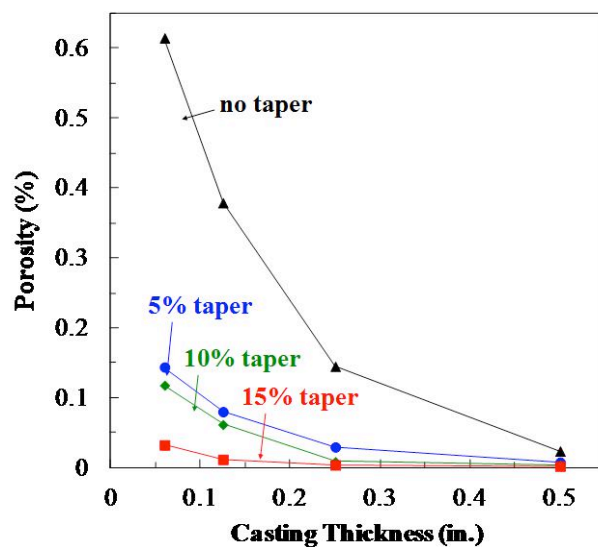


Figure 4. Effect of casting thickness and taper angle on porosity level.

Figure 4 summarizes the relationship between average porosity level in a plate with different casting wall thickness and taper. Such information can be used as a reference for casting process engineers. In order to make castings with an accepted level of average plate porosity, a corresponding optimal part design is needed. For example for a plate casting with the dimension of 8" long and 1.8" wide, if the acceptable level of average plate porosity is 0.2%, the taper has to be larger than 5% for wall thickness less than 0.1 inch. On the other hand, if the wall thickness is greater than quarter inch, taper is not necessary to meet this porosity specification level.

The authors are also in the process of assessing the accuracy, verification and validation of the POROS=1 + Ny^* model as applied to more complex casting geometries and processes. Results for these more detailed casting geometries will be discussed in future publications.

4. Conclusions

The dimensionless Niyama (Ny^*) model is integrated with the ProCAST POROS=1 model, where this integrated model can accurately predict both macro-and micro-shrinkage porosity during solidification of superalloy castings. The integrated model is validated by comparing modeled results against measured porosity for several Ni-based superalloy equiaxed castings that have different alloy chemistries and tapered plates with different configurations. The simulation results agree well with experimental measurements for the geometries presented in this paper.

Acknowledgements

The efforts reported under this paper are a direct result of funding provided under the US Government supported Metals Affordability (MAI) Program called HOW-5 (Contract # FA8650-11-2-5229 – Agreement Order 29). Technical Leadership and Oversight of the HOW-5 project were provided by Steven Turek and Jason Blake of AFRL, Wright Patterson Air Force Base, Dayton, OH whose efforts and inputs to enhance the HOW-5 projects technical efforts are greatly appreciated. The authors also wish to thank the MAI Technical Oversight Committee (TOC) and MAI Program office for their support, guidance and review of the HOW-5 program that this porosity modeling improvement effort is a part of.

References

- [1] Carlson K D and Beckermann C 2009 *Metallurgical and Materials Transaction A* **40A** 163-175
- [2] Campbell J, Castings, Butterworth-Heinemann, Oxford, United Kingdom, 1991
- [3] Kuznetsov A V and Vafai K 1995 *International Journal of Heat and Mass Transfer* **38** 2557-2567
- [4] Sigworth G K and Wang C 1993 *Metallurgical Transactions B* **24B** 349-364
- [5] Poirier D R, Yeum K and Maples A L 1987 *Metallurgical Transactions A* **18A** 1979-1987
- [6] Combeau H, Carpentier D, Lacaze J and Lesoult G 1993 *Materials Science and Engineering* **A173** 155-159
- [7] Sung P K, Poirier D R, Felicelli S D, Poirier E J and Ahmed A 2001 *Journal of Crystal Growth* **226** 363-377.
- [8] Zhu J D and Ohnaka I 1991 *Modeling of Casting, Welding and Advanced Solidification Processes V* 435-442
- [9] Sabau A and Viswanathan S 2002 *Metallurgical and Materials Transactions B* **33B** 243-255
- [10] See D, Atweed R C and Lee P D 2001 *Journal of Materials Science* **36** 3423-3435
- [11] Atwood R C and Lee P D 2002 *Metallurgical and Materials Transactions B* **33B** 209-221.
- [12] Lee P D, Atwood R C, Dashwood R J and Nagaumi H 2002 *Materials Science and Engineering* **A328** 213-222
- [13] Niyama E, Uchida T, Morikawa M and Saito S 1982 *AFS Cast Met. Res. J.* **7** 52–63
- [14] Felicelli S D, Poirier D R and Sung P K 2000 *Metallurgical and Materials Transactions B* **31B** 1283-1292
- [14] Anyalebechi P N 1998 *Light Metals* 827-842
- [15] Kubo K and Pehlke R D 1985 *Metallurgical Transactions B* **16B** 359-366
- [16] Guo J, Makinde A and Bewlay B 2009 *Modeling of Casting, Welding, and Advanced Solidification Processes – XII*, Edited b: Cockcroft S L and Maijer D M, TMS, pp. 337-344
- [17] Niyama E, Uchida T, Morikawa M and Saito S 1982 *AFS Cast Met. Res. J.* **7** 52–63